

## Corrosion Behaviors of Transition Metals in Liquid Na and LBE: A First-principles Study

Jeong-Hwan Han and Takuji Oda\*

Department of Nuclear Engineering, Seoul National University, 1, Gwanak-ro Gwanak-gu, Seoul 08826, Republic of Korea

\*Corresponding author: oda@snu.ac.kr

### 1. Introduction

Liquid metals play an important role in the development of generation IV reactors, which can be a solution to reduce the burden on the environment by burning up the spent nuclear fuel generated in light-water reactors. For instance, liquid sodium (Na) and lead (Pb) have been regarded as promising candidates for coolants in fast-neutron reactors. Liquid lead-bismuth eutectic (LBE) has been studied to be used as a coolant and neutron spallation source in accelerator-driven systems (ADSs) because of its high neutron spallation yield characteristic.

One of the important material issues that must be well understood for the realization of fast reactors is the corrosion of structural materials, which consist mainly of 3d transition metals such as Fe, Cr, and Ni. It is well known that liquid LBE and Pb greatly corrode steels and liquid Na has long-term and local corrosion problems. The corrosion mechanism in liquid metals is different from that in aqueous liquids. It has been reported that the metallic materials in liquid metals are corroded by (i) the atomic dissolution and (ii) mass transfer due to the formation of binary and ternary corrosion compounds with non-metallic impurities present in liquid metals or bulk solids [1]. The corrosion by atomic dissolution and mass transfer by chemical reactions causes the bulk and local corrosion, respectively.

Scientific understanding of why corrosion in liquid LBE and Na mainly proceeds in a bulk and local way, respectively, is expected to help develop corrosion prevention measures. However, there is still lack of knowledge about the reasons for the corrosion characteristics in liquid metals. To find an answer for this, deep understanding of the physiochemical states of 3d transition metal impurities in liquid LBE (*p*-electron liquid metal) and Na (*s*-electron liquid metal) would be needed.

As a useful tool for evaluating physiochemical states in detail, the present study uses quantum mechanical calculations based on the density functional theory (DFT) to perform the first-principles molecular dynamics (FPMD) simulations of liquid LBE and Na at 1000 K. Physiochemical properties of Fe, Cr, and Ni such as electronic density of states (DOS), magnetic moment, and charge state are evaluated.

### 2. Computational details

FPMD simulations of liquid LBE [2] and Na [3] were performed by Vienna *ab initio* simulation package (VASP) code [4] based on the DFT. The Perdew-Burke-Ernzerhof (PBE) functional of the generalized gradient approximation (GGA) was used. The energy cutoff of 300 eV was chosen to represent the electronic wave functions of the valence electrons. For Pb, Bi and Na,  $6s^26p^2$ ,  $6s^26p^3$ , and  $3s^1$  valence electrons were treated, respectively. The projected augmented wave (PAW) method was applied to address the effect of core electrons. The convergence criterion of energy in the electronic optimization step was  $10^{-6}$  eV. The band energy was evaluated by sampling over the  $2 \times 2 \times 2$  Monkhorst-Pack grid, leading to 4 irreducible *k*-points, and by using Methfessel-Paxton's smearing method of the 1<sup>st</sup> order with 0.2 eV smearing width. The spin polarization was considered.

For liquid LBE, the system composed of 45 Pb atoms and 57 Bi atoms was prepared to simulate the eutectic composition (44.1% Pb atomic concentration). The simulation results of liquid LBE have already been published [2]. For liquid Na, 102 atoms were prepared in the system. The periodic boundary conditions were applied in all cases. The FPMD simulations were performed at 1000 K in the canonical ensemble (NVT) with a Nosé thermostat for temperature control. 15 ps and 20 ps simulations were performed with a time step of 4 fs and 1.2 fs for liquid LBE [2] and Na [3], respectively. After the simulations, one solvent atom was replaced with a 3d metal impurity such as Fe, Cr, and Ni. Another 10 ps and 30 ps simulations were performed for liquid LBE [2] and Na systems containing one impurity, respectively. Since there was only one impurity in each system, interactions between impurities were not considered in these simulations.

### 3. Results and discussion

#### 3.1. Density of states (DOS)

The electronic DOSs of pure liquid LBE [2] and Na are presented in Fig. 1. The energy level are shifted so that the Fermi energy level lies at 0 eV. In Fig. 1(a) of the DOS of liquid LBE [2], there are 6s band and 6p band separately with an energy gap of 1.2 eV. As shown in Fig. 1(b), DOS of liquid Na is mainly composed of 3s band below the Fermi energy level.

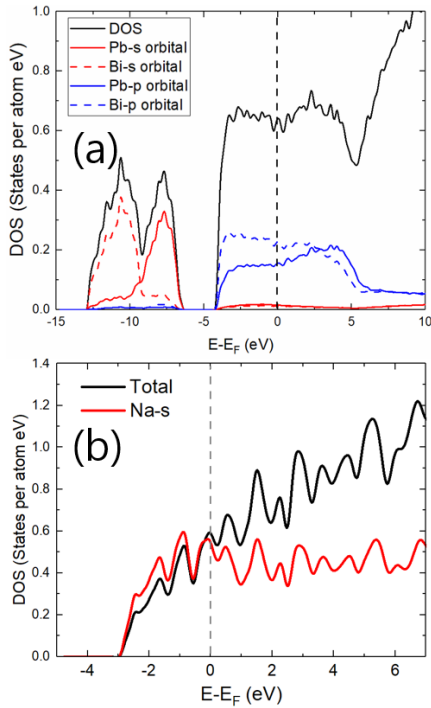


Fig. 1. The total DOS of (a) liquid LBE [2] and (b) Na.

To assess the electronic properties of Fe, Cr, and Ni, site-projected DOS of impurities in liquid LBE [2] and Na are presented in Fig. 2. The site-projected DOSs of impurities consist of the 4s and 3d orbitals.

In Fig. 2, for the 4s orbitals of impurities, a broadband overlapping the DOS of solvent atoms are observed for both liquid metal cases. It indicates that the 4s orbitals partly have metallic bonding with solvent atoms. While two sharp 4s peaks are observed in liquid LBE system, there is one sharp 4s peak in liquid Na system. Two 4s peaks observed in liquid LBE indicate that the 4s orbitals interact with surrounding LBE atoms in a covalent way consisting of a bonding and antibonding. In contrast, one sharp 4s peak in liquid Na indicates that there is ionic-type bonding, which will be addressed in Section 3.3.

For further investigation, with focusing on Ni impurity, the isosurface of charge density at the first peak position of Ni-4s band in liquid LBE and Na are visualized in Fig. 3(a) [2] and 3(c), respectively. In Fig. 3(a), the iso-charge surface near the Ni atom clearly shows the bonding orbitals between Ni-4s orbitals and surrounding LBE-6p orbitals. In Fig. 3(c), the isosurface does not exhibit bonding orbitals between Ni-4s orbitals and surrounding Na-3s orbitals.

For DOS of the 3d orbitals in Fig. 2, it can be seen that the spin-polarization is mainly induced by the 3d orbitals. It is due to the localization characteristics of d orbitals. Thus, quantifying the degree of spin-polarization helps to understand the properties of the 3d orbital interactions.

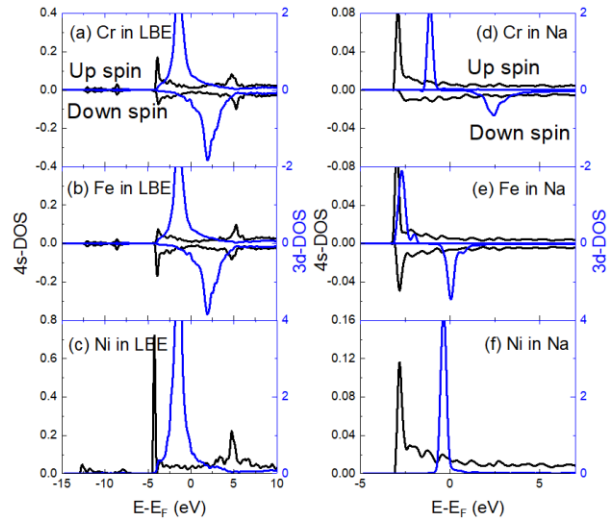


Fig. 2. The site-projected DOS of Cr, Fe, and Ni (a)-(c) in liquid LBE [2] and (d)-(f) liquid Na.

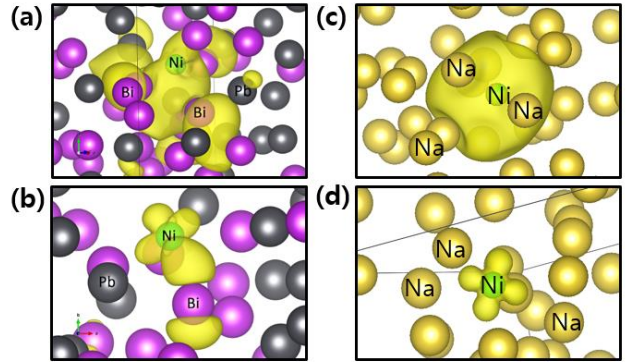


Fig. 3. The isosurface of charge density of Ni-4s and Ni-3d orbitals at the first peak DOS position (a)-(b) in liquid LBE [2] and (c)-(d) liquid Na.

### 3.2. Magnetic moment

The magnetic moment is the degree of spin-polarization measured by subtracting the number of occupied down-spin electrons from that of occupied up-spin electrons. Since there is no spin-polarization in pure liquid LBE [2] and Na [3], the system magnetic moment can be considered to be mainly due to the 3d orbitals.

As reported in our previous study [2], if the 3d orbitals interact strongly with surrounding orbitals, orbital energy levels are expected to be largely split. It indicates that an energy gain by the exchange energy is not enough to overcome the energy difference between the split energy levels, leading to the non-spin-polarization. In contrast, when the 3d orbitals weakly interact with surrounding orbitals, an energy gain by the exchange energy is sufficient to overwhelm the energy difference between the split energy levels, resulting in spin-polarization. In other words, the decrease and increase of the magnetic moment indicate that the

environment becomes chemically favorable and unfavorable for the  $3d$  orbitals, respectively.

Table I: The magnetic moment of Cr, Fe, and Ni in a vacuum, liquid LBE [2] and Na.

Mag. Mom. ( $\mu_B$ )	Cr	Fe	Ni
Vacuum	6.00	4.00	2.00
Liquid LBE [2]	3.63	2.40	0.00
Liquid Na	5.08	3.06	0.00

Table I summarizes the magnetic moment results of Cr, Fe, and Ni in a vacuum, liquid LBE [2] and liquid Na systems. When the system changes from a vacuum to liquid LBE, there is significant reduction in the magnetic moment, while the degree of reduction in the magnetic moment is small when the system changes from a vacuum to liquid Na. Therefore, it can be expected that the  $3d$  orbitals are more chemically stable in liquid LBE than in liquid Na. It agrees well with the experimental observation that the liquid LBE is more corrosive to structural metals than is liquid Na [5].

For Ni atom, the degree of decrease in the magnetic moment is the same when the system changes from a vacuum state to two liquid metals. Thus, the degree of interactions is further checked by visualization of the isocharge surface in Fig. 3(b) and 3(d). In liquid LBE, the  $3d$  orbitals strongly interact with the Bi- $6p$  orbitals as shown in Fig. 3(b). In liquid Na, on the other hand, there is no clear feature indicating that the  $3d$  orbitals strongly interact with surrounding Na- $3s$  orbitals, as shown in Fig. 3(d).

### 3.3. Charge state

The charge states of Cr, Fe, and Ni in liquid LBE [2] and Na were evaluated by the Bader analysis [6], in which the charge density is integrated within a volumetric area compared to the so-called zero-flux electron charge density.

Table II: The charge states of Cr, Fe, and Ni in liquid LBE [2] and Na.

Charge states (in $e$ )	Cr	Fe	Ni
Liquid LBE [2]	0.36	-0.01	-0.28
Liquid Na	-1.66	-1.76	-2.07

In Table II, it can be seen that the  $3d$  transition impurities easily gain electrons in liquid Na system. It is because of the small electronegativity of Na. This large electron transfer would cause the ionic-type bonding property in liquid Na, as observed in the  $4s$ -DOS of  $3d$  transition impurities in Fig. 2.

### 3.4. Prediction of corrosion mechanisms

In the case of liquid LBE ( $p$ -electron liquid metal), the  $3d$  transition metal elements strongly interact with  $6p$  electrons of solvent atoms, specifically  $4s$ - $6p$  and  $3d$ - $6p$  interactions [2]. As a result, the energy difference between an atom in a solid crystal (e.g. fcc Ni) and an atom dissolved in liquid LBE becomes relatively small. Thus, the main corrosion mechanism is atomic dissolution dominant corrosion. Therefore, the physical separation by the oxide film and Al-coating [6] can be the best way to prevent the bulk corrosion caused by atomic dissolution.

In the case of liquid Na ( $s$ -electron liquid metal), the interactions between a  $3d$  transition metal impurity and Na atoms are not strong enough to lead to atomic dissolution dominant corrosion. Specifically,  $4s$ - $3s$  and  $3d$ - $3s$  interactions are weak. Instead, the local corrosion due to the formation of chemical compounds could be the major cause of corrosion. Because the  $3d$  transition metals can readily obtain electrons from solvent atoms, high oxidation compounds can be chemically stable and formed, if they meet nonmetallic impurities. In experiment [7], it has been reported that high oxidation compounds such as  $\text{Na}_3\text{FeO}_4$  (V) and  $\text{NaCrO}_2$  (III) are formed, under a non-negligible concentration of nonmetallic impurities. Therefore, reducing the concentrations of nonmetallic impurities as low as possible is the best way to prevent the local corrosion induced by the formation of additional chemical compounds.

## 4. Conclusion

In the present study, the chemical states of the  $3d$  transition metal impurities such as Fe, Cr, and Ni dissolved in liquid LBE and Na were analyzed to understand the corrosion characteristics of structural metals. The FPMD simulations based on the DFT were performed to estimate the electronic DOS, magnetic moment, and charge state of impurities. We found that there are strong  $4s$ - $6p$  and  $3d$ - $6p$  interactions between  $3d$  impurities and liquid LBE. Relatively, the  $4s$ - $3s$  and  $3d$ - $3s$  interactions between  $3d$  impurities and liquid Na are weak. The charge states of Cr, Fe, and Ni are largely negative in liquid Na. As a result, we suggest that strong interactions between  $3d$  impurities and liquid LBE cause the atomic dissolution dominant corrosion. In the case of liquid Na, relatively weak interactions between  $3d$  impurities and liquid Na and large negative charge states of  $3d$  impurities promote mass transfer dominant corrosion by the formation of chemical compounds.

## 5. Acknowledgement

The present study was supported by National Research Foundation (NRF) of Korea under Nuclear

Research & Development Program by BK 21 plus project of Seoul National University. The computer resources and technical supports have been provided by the National Institute of Supercomputing and Network at the Korea Institute of Science and Technology Information (Project-ID: KSC-2017-C2-0034).

## REFERENCES

- [1] M. Li, K. Natesan, Y. Momozaki, D.L. Rink, W.K. Soppet, and J.T. Listwan, Report on sodium compatibility of advanced structural materials, ANL-ARC-205, 2012.
- [2] J. Han, and T. Oda, Chemical states of 3d transition metal impurities in a liquid lead-bismuth eutectic analyzed using first-principles calculations, *Phys. Chem. Chem. Phys.*, Vol. 19, No. 15, pp. 9945-9956, 2017.
- [3] J. Han, and T. Oda, Performance of exchange-correlation functionals in density functional theory calculations for liquid metal: A benchmark test for sodium, *J. Chem. Phys.*, Vol. 148, No. 14, pp. 144501-(1-9), 2018.
- [4] G. Kresse, and J. Furthmüller, Efficient iterative schemes for ab initio total-energy calculations using a plane-wave basis set, *Phys. Rev. B*, Vol. 43, No. 16, pp. 11169-11186, 1996.
- [5] G. Müller, G. Schumacher, A. Heinzl, A. Jianu, and A. Weisenburger, Handbook on lead-bismuth eutectic alloy and lead properties, materials compatibility, thermal-hydraulics and technologies, OECD-NEA handbook, Chapter 9, 2015.
- [6] J. Zhang, A review of steel corrosion by liquid lead and lead-bismuth, *Corrosion Science*, Vol. 51, No. 6, pp. 1207-1227, 2009.
- [7] S. Shin, J. Lee, J. Kim, and J. Kim, Mechanism of corrosion of 9Cr and 12C ferrite/martensitic steels under oxygen-saturated sodium, *Corrosion Science*, Vol. 112, No. C, pp 611-624, 2016.